Meas. Sci. Technol. **20** (2009) 084028 (5pp) doi:10.1088/0957-0233/20/8/084028

Size effects on the strength of nanotube bundles

Nicola Pugno[1], **Federico Bosia**[2] **and Alberto Carpinteri**[1]

[1] Department of Structural Engineering and Geotechnics, Politecnico di Torino, Corso Duca degli Abruzzi 24, 10129 Torino, Italy
[2] Department of Theoretical Physics, Università di Torino, Via Giuria 1, 10125 Torino, Italy

E-mail: nicola.pugno@polito.it, fbosia@to.infn.it and alberto.carpinteri@polito.it

Received 27 November 2008, in final form 2 February 2009
Published 30 June 2009
Online at stacks.iop.org/MST/20/084028

Abstract
We numerically investigate the scaling of mechanical properties of carbon nanotube bundles, with the objective of evaluating the potential characteristics of large-scale structures. The simulations are carried out using a fibre bundle model adapted at various size scales according to a self-similar scheme. Scaling of both strength and Young's modulus is analysed, comparing results for defective and non-defective bundles, i.e. in the absence or in the presence of voids. Various types of defects are considered, with different size, shape, density and distribution. Analytical laws are also proposed and compared to numerical results.

Keywords: carbon nanotubes, mechanical properties, scaling, fibre-bundle models

(Some figures in this article are in colour only in the electronic version)

1. Introduction

Carbon nanotube (CNT) bundles are potentially extremely interesting for engineering applications, due to the density, elastic modulus and especially mechanical strength that one can achieve [1]. Particularly ambitious structures such as a space elevator megacable [2], or 'super-bridges', i.e. kilometre-long suspended bridges, could be conceived exploiting the unique properties provided by CNT technology.

Many experimental studies exist for the evaluation of the mechanical characteristics of CNTs or CNT yarns, however numerical studies clearly become indispensable when predictions are to be made for full-scale structures. Due to the number of orders of magnitude involved, which can be up to 10 in the case of super-bridges or even 15 in the case of the space elevator megacable, problems often emerge due to the computing time or complexity involved. Inevitably, a statistical approach is called for, and the issue is then to consider all relevant parameters and to choose appropriate approximations for the problem to be analysed. In this respect, the role played by defects in the structure at various levels is of the utmost importance, especially in the determination of the final bundle strength.

To address these issues, we describe in this paper a numerical procedure, based on a fibre-bundle-model (FBM) approach, specifically developed to carry out multiscale simulations for CNT-based cables and estimate relevant mechanical characteristics, such as Young's modulus, strength or released elastic energy during damage progression, and evaluate the scaling of these properties with cable size.

The paper is organized as follows: the adopted FBM model and multiscale simulation procedure are described in section 2; numerical results are presented in section 3, and the conclusions and outlook are given in the final section.

2. Numerical model and multiscale approach

2.1. Fibre bundle model

Simulations are carried out using a recently developed simulation code for the description of damage progression and acoustic emission (AE) in materials [3]. The simulation code is based on an equal-load-sharing FBM approach [4], with randomly assigned (Weibull-distributed) fibre strengths σ_{Cij}. The specimen is modelled by adopting a discretization in N_x 'bundles' of N_y fibres (corresponding to CNTs or CNT bundles), and by applying at every time step the analytically calculated local loads deriving from an increasing externally applied stress $\sigma(t)$. An AE event is generated whenever this local stress exceeds the assigned fibre peak stress. In this

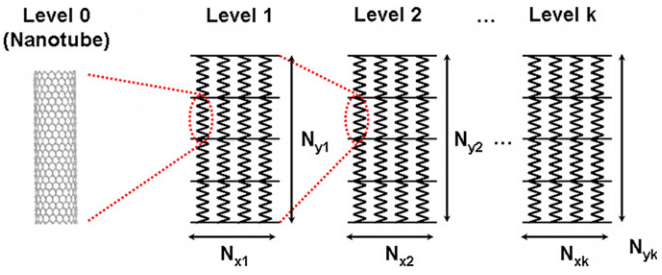

Figure 1. The hierarchical structure in multiscale simulations.

case, the corresponding fibre stiffness k_{ij} is set to zero and the related section (or bundle) undergoes a corresponding stiffness reduction.

Energy dissipation owing to the formation of new fracture surfaces at each AE event is also accounted for in the formulation: energy balance requires that the variation of the total potential energy $\Delta U_{ij}(t)$, when an AE event occurs at the location $(i,\ j)$, be compensated by the kinetic energy $\Delta T_{ij}(t)$, released in the form of a stress wave, and dissipated energy $\Delta\Omega_{ij}(t)$, in the formation of a crack surface at micro- or meso-scale [5]. Thus, we can write

$$\Delta U_{ij}(t) + \Delta T_{ij}(t) + \Delta\Omega_{ij}(t) = 0. \tag{1}$$

The potential energy variation $\Delta U_{ij}(t)$ is related to the imposed displacement $x(t)$ and the overall specimen stiffness variation $\Delta K_{ij}(t)$ occurring in correspondence with the AE event:

$$\Delta U_{ij}(t) = \tfrac{1}{2}x(t)^2\Delta K_{ij}(t) \tag{2}$$

while the dissipated energy $\Delta\Omega_{ij}$ is assumed to be proportional to the newly created crack surfaces A_{ij}:

$$\Delta\Omega_{ij} = G_C A_{ij}, \tag{3}$$

where G_C is the critical strain energy release rate of the material. The surfaces A_{ij} can be considered constant as a first approximation. At the lowest simulation level, these correspond to CNT cross sections (see section 2.2).

2.2. Multiscale procedure

In order to tackle the size scales involved in the modelization of CNT megacables, spanning up to ∼15 orders of magnitude from CNT (∼10^{-7} m) to megacable lengths, the FBM outlined above must be modified to accommodate multiscale simulations. The cable is therefore modelled as a N_{xk} by N_{yk} ensemble of subvolumes, arranged in parallel sections, as shown in figure 1. Each of the (primary) subvolumes is in turn constituted by $N_{x(k-1)}$ by $N_{y(k-1)}$ (secondary) subvolumes, arranged in parallel as before. This scheme is applied for k 'generations', down to a level 1 subvolume, which is constituted by a N_{x1} by N_{y1} arrangement of 'springs', representing the actual CNTs (figure 1). Here, we choose to adopt a scale-invariant approach, whereby the simulated structure appears the same at any given scale level (i.e. the length/width ratio is constant), and therefore choose $N_{x1} = N_{x2} = \cdots = N_{xk} = N_x$ and $N_{y1} = N_{y2} = \cdots = N_{yk} = N_y$. Overall, the cable is constituted by a total number of CNTs given by $N_{\text{tot}} = (N_x\ N_y)^k$.

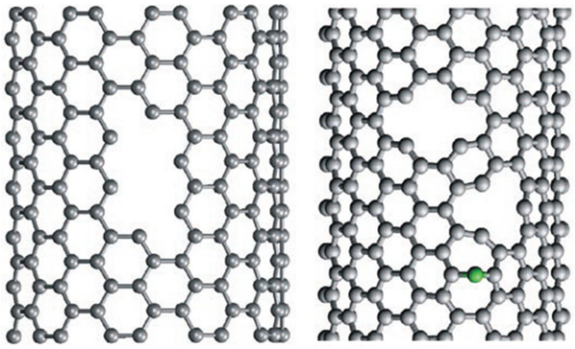

Figure 2. Examples of defects in a CNT structure (from [9]).

The numerical procedure is outlined in detail in [6]. Essentially, input mechanical properties at level 1 are directly estimated from nanotensile tests of CNTs [7]; level 1 output is considered as the input for the level 2 (after averaging over thousands of simulations for reliable statistics), and so on up to level k, corresponding to the final structure. Thus, various hierarchical levels are used to span lengths from that of a single CNT of about 100 nm to thousands of kilometres.

2.3. Presence of defects

As explained above, any numerical simulation regarding the mechanical characteristics of CNTs or CNT bundles without considering the role of defects would be unrealistic [8]. Defects can occur both at the atomic level (see figure 2) and at larger size scales, when there is the presence of single fractured CNTs or fractured CNT bundles. These defects (or 'voids') can be introduced in the simulations by setting local fibre stiffnesses k_{ij} to zero at selected locations and levels.

Two types of defects are considered:

(I) randomly assigned, uniformly distributed, introduced alternatively at levels 1 to k, in a percentage of 10%. Changing the simulation level at which voids are introduced amounts to considering the same defect concentrations, but in different agglomerations (i.e. from evenly distributed, at level 1, to unevenly distributed, at level k).

(II) (a) point, (b) circular and (c) line defects in the CNT bundle structure, all of which are introduced at level 1. This simulates the presence of medium-sized flaws or actual cracks in the structure.

3. Numerical results

3.1. Stress–strain behaviour

The first simulation is carried out at the CNT level, i.e. the 'fibres' in the first-generation subvolume are $L_0 = 10^{-7}$ m in length. This length value is not necessarily the CNT length, rather it represents a sort of 'correlation length', i.e. the distance beyond which a CNT rupture does not influence ruptures in other bundles. The fibres are $w_0 = 10^{-9}$ m in width, their Young's modulus is $E_0 = 10^{12}$ Pa and their strength

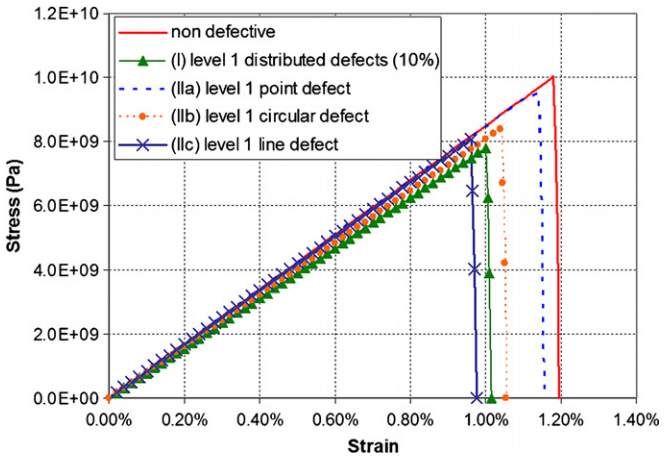

Figure 3. Stress–strain behaviour for different defect types.

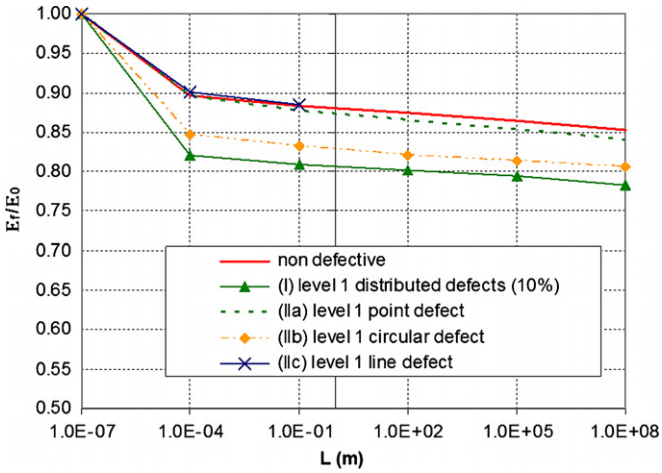

Figure 4. Scaling of CNT cable stiffness.

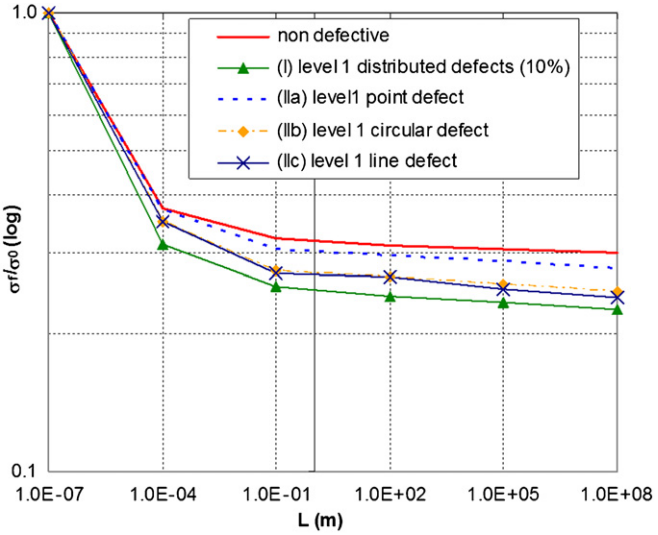

Figure 5. Scaling of CNT cable strength.

σ_{f0} is randomly assigned, based on the nanoscale Weibull [7] distribution:

$$P(\sigma_{f0}) = 1 - \exp[-(\sigma_{f0}/\sigma_0)^m], \tag{4}$$

where P is the cumulative probability and experimentally for CNTs $\sigma_0 = 34$ GPa and $m \approx 3$. This distribution accounts for statistical variations in the CNT strength that are to be expected for various reasons, including the presence of defects, as seen in figure 2. The strength σ_{f1} of the first-generation fibre bundle (whose length is $L_1 = L_0 N_{y1}$) is then derived as the average value of those deriving from a large number of repeated simulations (typically from 10^3 to 10^4), each with different randomly assigned local strengths, so as to build reliable statistics. In contrast, the strengths of the fibre bundles at levels 2 upwards (σ_{f2} to σ_{fk}), as explained above, are directly deduced from the numerically simulated distribution of strengths obtained at the previous level in each case. The strength σ_{fk} coincides with the final strength σ_f of the considered structure. In all simulations, the end-to-end connections between CNTs or CNT bundles (fibres in the model) are considered to have a strength comparable to that of a CNT or CNT bundle itself, assuming a long enough overlap length. Clearly, this could lead to an overestimate of the cable strength, i.e. we are estimating upper bound values for cable strength. Results are presented in figure 3 for simulations with $N_y/N_x = 25$, for defective and non-defective CNT bundles. Level 1 defect types (I) and (II) (see section 2.3) are considered.

The presence of defects affects stress–strain curves principally in their ultimate stress and strain values, although some variation in the stiffness is visible. Ultimate strains vary from 0.98% to 1.2% depending on the type of defect considered. All curves display brittle failure, as is expected from the type of strength distribution obtained numerically at this level.

3.2. Scaling of stiffness and strength of CNT bundles

The procedure outlined in section 2 allows us to study the scaling of stiffness and strength with CNT cable length, as well as to evaluate the influence of the presence of defects. Scaling is assessed over 15 orders of magnitude, from 10^{-7} m to 10^8 m (the latter being the space elevator megacable length), although only values of up to $\sim 10^3$ m are of practical interest for civil engineering applications. Figure 4 shows results for the scaling of the normalized cable stiffness E/E_0 and figure 5 shows those for the normalized cable strength σ_f/σ_0. Both for stiffness and strength, there is a reduction with increasing cable length. The main decrease occurs for small lengths ($<10^{-4}$ m) and then continues with an almost linear (in log scale) drop-off for larger abscissae. The reduction with increasing cable length is particularly significant for the strength (80–90% over the 15 orders of magnitude), whilst the stiffness decreases only about 15–20% over the same length range.

As already mentioned above, the presence of defects causes a non-negligible decrease in cable stiffness, with a 9% overall reduction in the case of a randomly distributed 10% void content. In this case, the effect of defect clustering is less pronounced, i.e. the stiffness reduction in the case of clustered circular defects is virtually the same as that for randomly

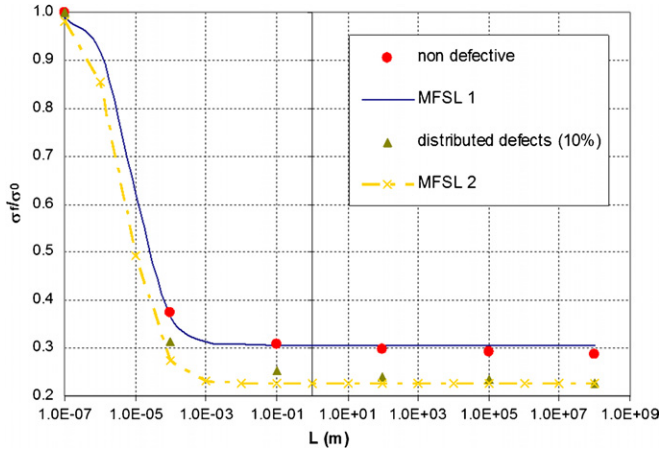

Figure 6. Comparison of analytical laws with numerical results (non-defective cable).

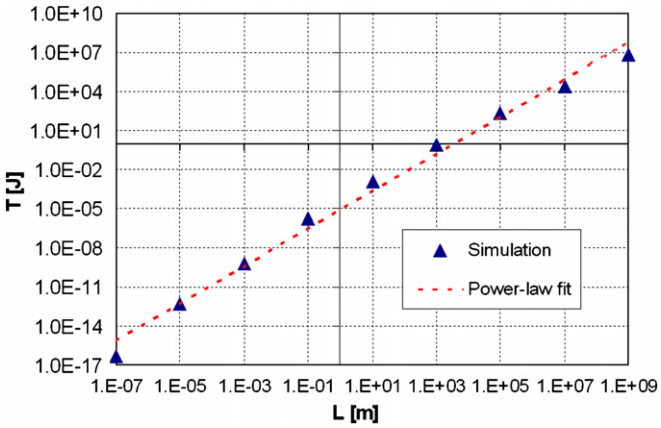

Figure 7. Scaling of released energy.

distributed defects. On the other hand, the presence of defects has a more consistent effect on the decrease of cable strength, with a further 13% reduction with respect to the non-defective value in the case of distributed defects, and a 29% reduction in the case of clustered circular defects. These simulations show how defects of non-negligible size have a more pronounced effect in reducing cable strength if compared to smaller defects with the same overall concentration, whereas in the case of the cable stiffness, it is mainly the defect concentration that plays a role. In general, defect clustering emphasizes the strength reduction.

3.3. Analytical laws for the scaling of strength

Given the decaying behaviour of σ_f versus L obtained from simulations, it is important to try and fit the data with simple analytical scaling laws. Various laws exist in the literature, and one of the most well-known is the multifractal scaling law (MFSL) originally proposed by Carpinteri [10, 11], and recently modified by Pugno towards the nanoscale [12]:

$$\frac{\sigma_f}{\sigma_{\text{nano}}} = \sqrt{\frac{\left(\frac{\sigma_{\text{nano}}}{\sigma_{\text{mega}}}\right)^2 - 1}{lS/V + 1}} + 1, \tag{5}$$

where S and V are the surface and volume of the considered structure, respectively, σ_{nano} is its nanostrength, σ_{mega} is its megastrength and l is a characteristic internal length. Note that for self-similar structures and for $\sigma_{\text{nano}} \gg \sigma_{\text{mega}}$ this law corresponds to the MFSL. Here, we can choose σ_{nano} as the nanotube strength and σ_{mega} as a CNT cable strength obtained in simulations, i.e. $\sigma_{\text{nano}} = 34$ GPa and $\sigma_{\text{mega}} = 10.20$ GPa for a non-defective cable, and $\sigma_{\text{nano}} = 34$ GPa and $\sigma_{\text{mega}} = 7.68$ GPa for a cable with 10% distributed defects. Also, $S/V = 1/L$, whereas l remains a free fitting parameter. Results are shown in figure 6 for the two sets of data, 'non-defective' and 'distributed defects (10%)'. Each is compared to an analytical curve ('MFSL 1' and MSFL 2' curves) using equation (5), for the various L considered at the different hierarchical levels ($m = 2.7$). The best fit is obtained in both cases for $l = 5 \times 10^{-5}$ m, where the analytical curves are practically coincident with the simulated results. This can lead to an interpretation of l as a characteristic 'decay length', in analogy for example with decay times in nuclear physics, beyond which the structure undergoes a considerable part of the strength reduction.

Another analytical scaling law for σ_f can be obtained by considering the classical Weibull prediction, i.e.

$$\frac{\sigma_f}{\sigma_0} = kV^{-\frac{1}{m_1}}, \tag{6}$$

where V is the volume of the structure, calculated here as the sum of the volumes of the CNTs (or 'springs'), and k and m_1 are fitting constants. Coincidence of σ_f/σ_0 with numerical results for $L = L_1$ and $L = L_5$ is obtained for $k = 0.29$ and $m_1 = 45$. However the overall behaviour (not reported in the figure) does not match the numerical results, because the initial decrease is not sharp enough.

3.4. Scaling of released energy

Using the described multiscale simulation procedure, the scaling of the released elastic energy T up to CNT bundle fracture can also be determined as a function of the bundle length. Results are shown in figure 7. A power-law increase (linear behaviour in log–log scale) is found with a slope close to 1.5, similarly to previous results relative to different materials [3]. Results in figure 7, however, are obtained in a much greater length range, showing the advantages of the adopted multiscale simulation procedure.

4. Conclusions

We have presented numerical simulations based on a modified FBM approach with due consideration for energy dissipation and a multiscale procedure to determine scaling properties of CNT bundles in a wide length range. Analysed properties include strength, stiffness and released energy. The effect of defects on the bundle stiffness and strength is discussed. Results show consistent reductions of strength with cable length and, to a lesser extent, of stiffness, and in both cases the presence of defects is found to be non-negligible. Analytical

laws are proposed for the scaling of strength. Power-law type behaviour is found for energy scaling, similarly to existing experimental and numerical results in the literature, but in this case relative to a much greater length range. The numerical procedure shows promise and could in the future be used in specific detailed studies on CNT cable applications.

Clearly, the approach of considering only linear elastic behaviour up to rupture for the fibres in the model is a considerable simplification of the actual behaviour in CNT bundles, as results using the interatomic potentials indicate [13–15]. The presence of nonlinear effects (plastic behaviour) will therefore be included in the model in future work.

Acknowledgments

NP and AC are supported by the 'Bando Ricerca Scientifica Piemonte—2006'.

References

[1] Koziol K, Vilatela J, Moisala A, Motta M, Cunniff P, Sennett M and Windle A 2007 High-performance carbon nanotube fiber *Science* **318** 1892
[2] Edwards B C 2000 Design and deployment of a space elevator *Acta Astronautica* **10** 735
[3] Bosia F, Pugno N, Lacidogna G and Carpinteri A 2008 Mesoscopic modeling of acoustic emission through an energetic approach *Int. J. Solids Struct.* **45** 5856
[4] Cruz Hidalgo R, Kun F and Herrmann H J 2001 Bursts in a fiber bundle model with continuous damage *Phys. Rev.* E **64** 066122
[5] Carpinteri A and Pugno N 2005 Are the scaling laws on strength of solids related to mechanics or to geometry? *Nat. Mater.* **4** 421
[6] Pugno N, Bosia F and Carpinteri A 2008 Multiscale stochastic simulations as in-silico tensile testing of nanotube-based macroscopic cables *Small* **8** 1044
[7] Pugno N and Ruoff R 2006 Nanoscale Weibull statistics *J. Appl. Phys.* **99** 024301
[8] Zhang S, Mielke S L, Khare R, Troya D, Ruoff R S, Schatz G C and Belytschko T 2005 Mechanics of defects in carbon nanotubes: atomistic and multiscale simulations *Phys. Rev.* B **71** 115403
[9] Krasheninnikov A V and Banhart F 2007 Engineering of nanostructured carbon materials with electron or ion beams *Nat. Mater.* **6** 723
[10] Carpinteri A 1994 Fractal nature of material microstructure and size effects on apparent mechanical properties *Mech. Mater.* **18** 89
[11] Carpinteri A 1994 Scaling laws and renormalization groups for strength and toughness of disordered materials *Int. J. Solids Struct.* **31** 291
[12] Pugno N 2006 The role of defects in the design of space elevator cable: from nanotube to megatube *Acta Materialia* **55** 5269
[13] Zhang P, Huang Y, Geubelle P H, Klein P A and Hwang K C 2002 The elastic modulus of single-wall carbon nanotubes: a continuum analysis incorporating interatomic potentials *Int. J. Solid Struct.* **39** 3893–906
[14] Zhang P, Jiang H, Huang Y, Geubelle P H and Hwang K C 2004 An atomistic-based continuum theory for carbon nanotubes: analysis of fracture nucleation *J. Mech. Phys. Solids* **52** 977–98
[15] Wu J, Hwang K C and Huang Y 2008 An atomistic-based finite-deformation shell theory for single-wall carbon nanotubes *J. Mech. Phys. Solids* **56** 279–92